Proceedings of the ASME 2010 3rd Joint US-European Fluids Engineering Summer Meeting and 8th International Conference on Nanochannels, Microchannels, and Minichannels
FEDSM-ICNMM2010
August 1-5, 2010, Montreal, Canada

FEDSM-ICNMM2010-30539

AN EXPERIMENTAL STUDY OF FLOW PAST A DUAL STEP CYLINDER

Chris R. Morton
Mechanical and Mechatronics Engineering
University of Waterloo
Waterloo, Ontario, Canada

Serhiy Yarusevych
Mechanical and Mechatronics Engineering
University of Waterloo
Waterloo, Ontario, Canada

ABSTRACT

Flow past a dual step cylinder has been investigated using experimental flow visualization methods. The dual step cylinder model is comprised of a small diameter cylinder (d) and a large diameter cylinder (D) mounted at the mid-span of the small cylinder. The experiments have been performed for $Re_D = 1050$, $D/d = 2$, and a range of large cylinder aspect ratios (L/D). The focus of the study is on vortex shedding and vortex interactions occurring in the large and small cylinder wakes. A flow visualization study completed using hydrogen bubble technique and planar laser induced fluorescence has shown that the flow development is highly dependent on the aspect ratio of the large cylinder, L/D. The results identify four distinct flow regimes: (i) for $L/D \geq 17$, three vortex shedding cells form in the wake of the large cylinder, one central cell and two cells of lower frequency extending over about 4.5D from the large cylinder ends, (ii) for $7 < L/D \leq 14$, a single vortex shedding cell forms in the wake of the large cylinder, whose shedding frequency decreases with decreasing L/D, (iii) for $2 \leq L/D \leq 7$, vortex shedding in the wake of the large cylinder is highly three-dimensional, such that each vortex deforms while it is shed into the wake, (iv) for $0.2 \leq L/D \leq 1$, only small cylinder vortices are shed in the wake and often form vortex connections across the wake of the large cylinder.

INTRODUCTION

Fluid flow around cylindrical bodies has been the focus of a significant number of studies over the past several decades, e.g., Refs. [1-3]. The majority of previous investigations have been focused on a uniform circular cylinder, with a comprehensive review of the flow development given by Williamson [2]. In contrast, investigations involving more complex cylindrical geometries (e.g., step-cylinders, tapered cylinders, and free-end cylinders) are far less common. It has been shown that these geometries are associated with flow development similar to that for a uniform cylinder. In particular, the vortex shedding phenomenon is observed in the wake, however, due to the non-uniform geometry, wake vortex shedding occurs in distinct cells of constant shedding frequency. The vortex shedding characteristics depend strongly on the model geometry and the Reynolds number. For example, the wake of a single step cylinder has been shown to yield as many as three spanwise vortex cells, e.g., Refs. [4-6], one cell in the wake of the smaller diameter cylinder and two distinct cells in the wake of the larger diameter cylinder. For tapered cylinders, multiple vortex shedding cells develop across the span, e.g., Ref. [7]. For a free end or cantilevered cylinder, a lower frequency vortex shedding cell forms near the free end, and a higher frequency cell, similar to vortex shedding in the wake of a uniform circular cylinder, is observed away from the free end, e.g., Ref. [8].

The current investigation is focused on the flow development over dual step cylinders (Fig. 1). This geometry has been studied by Williamson [9] and Nakamura and Igarashi [10], however the investigations involved relatively small aspect ratio large cylinders ($L/D < 4$). Although the previous studies on dual step cylinders were not focused on wake vortex dynamics, due to similarities in geometry, the vortex shedding in the wake of a dual step cylinder is expected to be related to that for a single step cylinder and a free end cylinder.

For the single step cylinder geometry, previous experimental studies suggest that, vortex interactions take place in a wake region downstream of the step due to a mismatch between shedding frequencies of the large diameter (D) and small diameter (d) cylinders. For large diameter ratios ($D/d > 1.55$) and Re_D greater than about 100, vortex shedding occurs in three spanwise vortex shedding cells [4]. Dunn and Tavoularis [5] classify these cells as follows: (i) the S-cell, vortex shedding from the small cylinder; (ii) the L-cell, vortex shedding from the large cylinder; (iii) the N-cell, distinct vortex shedding in the region between the S-cell and N-cell. Flow visualization results by Dunn and Tavoularis [5] and Lewis and

Gharib [4] suggest that the N-cell is a cyclic phenomenon. That is, the formation of N-cell vortices interrupts periodically and then resumes after a few L-cell shedding cycles.

The wake of a cylinder with two free ends has been studied both experimentally and numerically, e.g., Refs. [11,12]. Previous results indicate a strong dependence of the flow topology on Re_D and the aspect ratio, L/D. Inoue and Sakuragi [12] completed a detailed numerical study of this flow at low Reynolds numbers, and identified different patterns of vortex shedding as a function of both Re_D and L/D. In particular, for L/D greater than about 20, three vortex shedding cells are detected across the cylinder span; one central cell and two end cells of lower frequency extending about 10D from each of the cylinder ends [12]. For a cylinder less than about 20D in length, a single vortex shedding cell is observed across the span. The shedding frequency of this single cell decreases with decreasing L/D until a transition to a distorted three-dimensional vortex shedding occurs for $L/D \leq 10$. At lower L/D ratios, the flow topology becomes highly dependent on the Reynolds number. For sufficiently small L/D, alternate shedding of counter-rotating vortex pairs may be seen in the wake [12].

The present study is motivated by the need for insight into dual step cylinder wake development. The objective is to investigate this flow for D/d = 2 and Re_D = 1050, identifying the effect of the large cylinder aspect ratio (L/D) on the wake vortex shedding.

NOMENCLATURE

D	=	large cylinder diameter
d	=	small cylinder diameter
f	=	vortex shedding frequency
f_L	=	vortex shedding frequency of the L-cell
f_{N1}	=	vortex shedding frequency of the N1-cell
f_{N2}	=	vortex shedding frequency of the N2-cell
f_{S1}	=	vortex shedding frequency of the S1-cell
f_{S2}	=	vortex shedding frequency of the S2-cell
L	=	span of the large cylinder
Re_D	=	Reynolds number, UD/ν
St	=	Strouhal number, fD/U
t	=	time
t*	=	dimensionless time, tf_{S1}
U	=	free-stream velocity
u, v, w	=	streamwise, transverse, and spanwise velocity components
X,Y,Z	=	streamwise, transverse, and spanwise coordinates
ρ	=	density
ν	=	kinematic viscosity

EXPERIMENTAL METHOD

All experiments were carried out in a water flume facility in the Fluid Mechanics Research Laboratory at the University of Waterloo. The 2.0 m long test section of the flume has a height of 1.2 m and a width of 1.2 m. During the experiments, the water level was maintained at 0.8 m, and the background turbulence intensity was less than 1%. The flow development over uniform, single step, and dual step cylinders was investigated. The cylinders were mounted between two endplates, following design recommendations of West and Fox [13]. The flume was operated at a free stream speed of 87mm/s, with a flow uniformity within 2.3%. Figure 2 shows the experimental arrangement of the dual step cylinder. The uniform and single step cylinders were tested in the same experimental arrangement.

To visualize wake vortices, a hydrogen bubble technique and planar Laser Induced Fluorescence (LIF) were employed. The flow was illuminated using a laser sheet generated by a 2W continuous wave laser. Hydrogen bubbles were produced on a thin (0.09 mm diameter) stainless steel wire. The wire was mounted approximately 0.2D upstream of the step cylinder along its entire span, similar to the arrangement used by Kappler et al. [14] for a uniform cylinder. With a DC voltage applied to the stainless steel wire, a continuous sheet of bubbles is generated in the X-Z plane. It was verified experimentally that buoyancy had a negligible effect on the motion of hydrogen bubbles.

For planar LIF visualization, Rhodamine dye was injected from a small probe placed about 20D upstream of the cylinder axis. The dye was illuminated in the X-Y plane to visualize wake vortex shedding, and in the X-Z plane to visualize flow near the step. When visualizing vortex shedding in the X-Y plane, the dye injection and hydrogen bubble systems were used simultaneously (Fig. 3). This allowed correlating the planar LIF images obtained in the X-Y plane to the spanwise development of wake vortices monitored in the X-Z plane. In addition, vortex cores were easier to identify in the planar images. For hydrogen bubble visualizations, spanwise vortices on one side of the wake were illuminated with a laser sheet positioned in the X-Z plane at $Y/D \approx 0.375$.

Flow visualization images were obtained with a Nikon D300 camera. In addition, another camera was used to record videos simultaneously with sequences of still images to aid in the identification of periodic phenomena in the wake.

RESULTS

The results have been divided into two sections. First, experimental results for flow past uniform cylinders and a single step cylinder are presented. In the second section, experimental data pertaining to flow past a dual step cylinder are discussed. All the results presented pertain to Re_D = 1050.

Flow Development over Uniform and Single Step Cylinders

Flow over uniform cylinders and a single step cylinder has been investigated experimentally by Morton and Yarusevych [6] in the same experimental facility. The two uniform cylinders investigated corresponded to the large (diameter, D) and the small (diameter, d) cylinders in the step cylinder

configuration (D/d = 2). Away from the end plates, parallel vortex shedding was observed in the wake of the uniform cylinders [6]. An analysis of video records revealed that, apart from the end cells which form within about 3-4 diameters from each endplate, the shedding frequency is constant along the span of the uniform cylinders, with St = 0.203 and St = 0.198 for the large and small cylinder, respectively [6]. These values are in agreement with previous experimental results reported by Norberg [3].

Flow visualization images presented in Fig. 4a and 4b show vortex shedding in the wake of a step cylinder. Agreeing with previous studies, e.g., Refs. [4,5], three vortex cells form in the wake. The S-cell forms in the wake of the small cylinder (Z/D>0). In the large cylinder wake, the N-cell forms near the step (Fig. 4b), bounded by the S-cell and the L-cell. The three cells are characterized by distinct vortex shedding frequencies, with the N-cell frequency being the lowest. This leads to complex vortex interactions at cell boundaries (Fig. 4b), investigated in detail in Ref. [6].

Flow Development over Dual Step Cylinders

Flow over a dual step cylinder was investigated for Re_D = 1050, D/d = 2, and $0.2 \leq L/D \leq 17$. The aspect ratio (L/D) was found to have a profound effect on wake vortex shedding. Four distinct flow regimes have been identified and are discussed in detail in this section. It should be noted that the bounds of L/D values associated with the identified regimes provide an approximate measure of the corresponding L/D ranges. Unless specified otherwise, the main vortex shedding cells in the wake of the large and small cylinders will be referred to as the L-cell and the S-cell, respectively.

L/D=17: The flow development over a dual step cylinder for L/D = 17 is illustrated in Fig. 5. Cellular vortex shedding is observed in the wake (Fig. 5a), with three vortex cells forming along the large cylinder span and a single vortex cell along the small cylinder. Evidently, the formation of the two distinct vortex shedding cells near the steps on the large cylinder side is similar to the N-cell formation in the wake of a single step cylinder [5]. Adopting the terminology introduced for a single step cylinder by Dunn and Tavoularis [5], the observed shedding pattern in the wake of a dual step cylinder can be classified as follows: (i) the S1-cell, vortex shedding from the small cylinder in the region $8 \leq Z/D \leq 13$, (ii) the N1-cell, vortex shedding from the large cylinder in the region $3 \leq Z/D \leq 8.5$, (iii) the L-cell, vortex shedding from the large cylinder in the region $-7.5 \leq Z/D \leq 7.5$, (iv) the N2-cell, vortex shedding from the large cylinder in the region $-8.5 \leq Z/D \leq -3$, and (v) the S2-cell, vortex shedding from the small cylinder in the region $-13 \leq Z/D \leq -8$. Figure 5b shows an approximate maximum extent of the identified cells as well as the corresponding shedding frequencies, estimated based on an analysis of video records. It should be noted that similar to the case of a uniform cylinder, end cells were observed near the end plates but are not shown in Fig. 5b.

The development of vortex shedding cells in the wake of the large cylinder is illustrated by sequences of flow visualization images shown in Figs. 6-8. Figures 6a, 7a, and 8a show nearly parallel vortex shedding in the wake of the large cylinder. Over time, vortices in the large cylinder wake become inclined towards the step at Z/D = 8.5 (Fig. 6b), at Z/D = -8.5 (Fig. 7b), or both steps (Fig. 8b). Eventually, a distinct vortex shedding cell, the N1-cell and/or N2-cell (Figs. 6c, 7c, 8c), appears near either of the two steps. The N-cell vortices move out of phase with the L-cell vortices until a vortex dislocation occurs (e.g., Z/D = 2 and X/D = 3 in Fig. 6c). Eventually, the N-cell vortices re-align in phase with the large cylinder vortices, and after a few L-cell shedding cycles, vortices are again shed parallel to the large cylinder axis, marking the beginning of the next N-cell cycle. An analysis of video records revealed that the cyclic development of the N1-cell (Fig. 6) and the N2-cell (Fig. 7) occurs typically in an alternating fashion. That is, an N1-cell cycle is followed by an N2-cell cycle. However, occasionally, N1 and N2 cells form simultaneously, as illustrated in Fig. 8. The results suggest that the flow topology in the wake of a dual step cylinder observed for L/D = 17 within $Z/D > 0$ and $Z/D < 0$ is similar to that observed for a single step cylinder. Moreover, for cylinders with two free ends, the numerical results of Inoue and Sakuragi [12] show similar cellular shedding, with lower frequency cells observed near the free ends for $L/D > 20$. Thus, it can be speculated that the observed wake development will persist for $L/D \geq 17$.

Due to the difference in vortex shedding frequencies between adjacent vortex cells, vortex dislocations occur at cell boundaries. Based on the results presented in Fig. 5b, the following transition regions between distinct cells along the span of the cylinder can be identified: (i) the S1-N1 cell region, $7.5 \leq Z/D \leq 8.5$, (ii) the N1-L cell region, $3 \leq Z/D \leq 7.5$, (iii) the N2-L cell region, $-7.5 \leq Z/D \leq -3.0$, and (iv) the S2-N2 cell region, $-8.5 \leq Z/D \leq -7.5$. Within these transition regions, vortex splitting occurs, resulting in intricate vortex connections. In the S1-N1 cell region, S1-cell vortices often form direct vortex connections with N1-cell vortices (Fig. 6b). In the N1-L cell region, N1-cell vortices frequently form direct connections with L-cell vortices (Fig. 6b and 6c). When N1-cell vortices are out of phase with L-cell vortices, they split into at least two vortex filaments, forming vortex connections with two consecutive L-cell vortices on the same side of the wake (Fig. 6b and 6c). Similar types of vortex interactions can be seen in Figs. 7a-c within the N2-L and S2-N2 cell regions.

Changes in the vortex shedding pattern along the span of the dual step cylinder at L/D = 17 are depicted in Fig. 9. The flow visualization images presented for $Z/D \geq 0$ illustrate typical flow patterns seen within the S1-cell (Fig. 9b), the S1-N1 cell region (Fig. 9c), the N1-cell (Fig. 9d), the N1-L cell region (Fig. 9e), and the L-cell (Fig. 9f). Periodic vortex shedding, similar to that observed for uniform cylinders, is seen within the S1-cell, N1-cell, and L-cell (Figs. 9b, 9d, and 9f). In contrast, within the cell transition regions, vortex interactions result in a dramatically different pattern (Figs. 9c and 9e). The

results presented in Fig. 9 are representative of the corresponding regions located at $Z/D \leq 0$.

7<L/D≤14: In this flow regime, vortex shedding from the large cylinder occurs in a single cell across the entire span. As shown in Fig. 10a, vortices in the large cylinder wake are shed parallel to the cylinder axis, and continue to form vortex connections with small cylinder vortices similar to those found for L/D = 17. For uniform flow past a cylinder with two free ends, Inoue and Sakuragi [12] observed a comparable flow regime for $10 < L/D < 20$.

Estimates of the shedding frequency of the three vortex shedding cells (S1-cell, L-cell, and S2-cell) were obtained based on the analysis of video record capturing over 100 L-cell shedding cycles. The S1 and S2-cell shedding frequencies were found to match the corresponding frequencies for L/D = 17 (Fig. 5b), while the L-cell shedding frequency decreases with decreasing L/D ratio: (i) L/D = 14, $f_L D/U = 0.193$, (ii) L/D = 10, $f_L D/U = 0.186$, and (iii) L/D = 7, $f_L D/U = 0.175$. Inoue and Sakuragi [12] report a similar trend for cylinders with two free ends.

Changes in the vortex shedding pattern along the span can be seen in Fig. 10, which shows three flow visualization images for L/D = 10. The images represent typical flow patterns seen within the S1-cell (Fig. 10b), the S1-L transition region (Fig. 10c), and the L-cell (Fig. 10d). Within the transition region between the S1 and L-cell, a distorted shedding pattern is observed (Fig. 10c). Vortex dislocations occur within the S1-L and S2-L transition regions, located within $4 \leq Z/D \leq 5$ and $-4 \leq Z/D \leq -5$, respectively. However, as the aspect ratio is decreased to L/D = 7, the S1-L and S2-L transition regions no longer remain in fixed Z/D ranges, marking the onset of another flow regime.

2≤L/D≤7: In this regime, vortex shedding persists in the wakes of the small cylinders but becomes difficult to identify in the wake of the large cylinder. The S1-L and S2-L transition regions are deflected towards the small cylinder near the steps. As can be seen in Fig. 11a, vortex shedding in the large cylinder wake cannot be adequately visualized with a laser sheet positioned at Y/D = 0.375, but its presence is evident in planar images (Figs. 11d-f). Spanwise development of large cylinder vortices (L-cell vortices) was visualized by repositioning the laser sheet to Y/D = 0.75. The flow visualization image sequence shown in Figs. 12a-c depicts large cylinder vortex shedding. In Fig. 12a, a large cylinder vortex can be seen at $X/D \approx 3.0$, $-2.5 < Z/D < 2.5$. In Fig. 12b, the same vortex has moved downstream to $X/D \approx 4$, $-1.5 < Z/D < 1.5$. As the spanwise extent of the vortex in the plane of visualization decreases with X/D, it can be conjectured that the vortex undergoes three-dimensional deformation. In Fig. 12c, this vortex can no longer be clearly identified at its expected downstream location $X/D \approx 5$. For laminar shedding from a cylinder with two free ends, similar three-dimensional deformation of the shed vortices was observed by Inoue and Sakuragi [12] for aspect ratios less than about 10. Inoue and Sakuragi [12] refer to this type of shedding as a hairpin shedding, as vortices attain a hairpin-like shape in the wake. However, in the present study pertaining to a turbulent shedding regime, the downstream development of the deforming L-cell vortices is likely to be influenced by the presence of small cylinder vortices as well as smaller scale structures.

Changes in the vortex shedding pattern along the span of a dual step cylinder can be seen in Figs. 11b-f, which show flow visualization images for L/D = 5. The images represent typical flow patterns seen within the S1-cell (Fig. 11b), the S1-L cell region (Fig. 11c), and the L-cell (Fig. 11d-f). In contrast with flow regimes observed for higher L/D, Figs. 11d-f illustrate intermittent shedding patterns within the L-cell. Figure 11d shows a planar shedding pattern similar to that observed in the wake of a uniform cylinder. Such a pattern is no longer observed in Figs. 11e and 11f, although these figures still show evidence of large scale vortices forming in the wake. Zdravkovich et al. [11], found a similar intermittent vortex shedding behaviour in the wake of a cylinder with two free ends for $2 < L/D < 8$, which was accompanied by large variations in vortex shedding frequency [11].

0.2≤L/D≤1: Figure 13 illustrates the flow development in this regime. As was confirmed by the analysis of video records, vortices are no longer detectable in the large cylinder wake. In Fig. 13a, S1 and S2-cell vortices can be seen in the wake at $X/D \approx 1$ and 3. The S-cell vortices in the region surrounding the large cylinder appear to form direct connections across the wake of the large cylinder. In Fig. 13b, the same vortex connection between S1 and S2-cell vortices can be seen farther downstream at $X/D \approx 4$. However, a dislocation occurs in Fig. 13c, where subsequent S-cell vortices at $X/D \approx 2.5$ do not connect across the large cylinder wake. A detailed analysis of video records revealed that S1 and S2 cell vortices form vortex connections across the large cylinder wake in an alternating fashion. It can be speculated that the observed vortex dislocations are linked to some periodic flow phenomenon. In comparison, Inoue and Sakuragi [12] found alternate shedding of counter-rotating vortex pairs for a cylinder with two free ends at $L/D \approx 1$ and $200 \leq Re_D \leq 300$.

Changes in the vortex shedding pattern along the span of the dual step cylinder at L/D = 1 are depicted in Fig. 14. The images represent typical flow patterns seen within the S1 and S2-cells (Fig. 14b), and in the wake of the large cylinder (Fig. 14c). Although a shear layer roll-up can be seen in Fig. 14c, no clear vortex shedding pattern is visible in the near wake.

CONCLUSIONS

Vortex shedding in the wake of a dual step cylinder was investigated experimentally for $Re_D = 1050$, D/d = 2, and $0.2 \leq L/D \leq 17$. The flow development was found to depend significantly on L/D ratio. For the cases investigated, four distinct vortex shedding regimes were identified.

For $L/D \geq 17$, the flow development near each of the two steps was similar to that found for a single step cylinder. Five distinct vortex shedding cells form in the wake: the S1-cell, the

N1-cell, the L-cell, the N2-cell, and the S2-cell. The N1 and N2-cells have the lowest of the five shedding frequencies and form in a region downstream of each step change in diameter on the large cylinder side. Due to the difference in shedding frequency between the five cells, vortex connections and dislocations are observed at cell boundaries.

For $7 < L/D \leq 14$, vortex shedding from the large cylinder occurs in a single cell across the entire span. Vortices in the large cylinder wake are shed nearly parallel to the cylinder axis and continue to form vortex connections with small cylinder vortices, similar to the vortex connections seen for higher aspect ratios. The shedding frequency of the L-cell in this flow regime decreases with decreasing L/D ratio.

For $2 \leq L/D \leq 7$, vortex shedding is highly three-dimensional. In particular, vortices initially form parallel to the cylinder axis, but in the near wake they deform substantially. Moreover, vortex shedding occurs intermittently in the wake of the large cylinder. It is speculated that this type of intermittency is similar to that observed by Zdravkovich et al. [11] in the wake of a cylinder with two free ends for $2 < L/D < 8$.

For $0.2 \leq L/D \leq 1$, the results suggest that spanwise vortices are no longer shed from the large cylinder. Downstream of the large cylinder dislocations occur between the two S-cells. It is speculated that these dislocations may be linked to some quasi-periodic phenomenon taking place in the large cylinder wake.

ACKNOWLEDGMENTS

The authors gratefully acknowledge the Natural Sciences and Engineering Research Council of Canada (NSERC) for funding of this work.

REFERENCES

[1] Gerrard, G.H., 1978, "The wakes of cylindrical bluff bodies at low Reynolds number," Philosophical Transactions of The Royal Society of London A **288**, pp. 351-382.

[2] Williamson, C.H.K., 1996, "Vortex dynamics in the cylinder wake," Annual Review of Fluid Mechanics **28**, pp. 477-539.

[3] Norberg, C., 2003, "Fluctuating lift on a circular cylinder: review and new measurements," Journal of Fluids and Structures **17**, pp. 57-96.

[4] Lewis, C.G., and Gharib, M., 1992, "An exploration of the wake three dimensionalities caused by a local discontinuity in cylinder diameter," Physics of Fluids A **4**, pp. 104-117.

[5] Dunn, W., and Tavoularis, S., 2006, "Experimental studies of vortices shed from cylinders with a step-change in diameter," Journal of Fluid Mechanics **555**, pp. 409-437.

[6] Morton, C.R., and Yarusevych, S., 2010, "A Combined Experimental and Numerical Study of Flow Past a Single Step Cylinder," Proceedings of ASME 2010 3rd Joint US-European Fluids Engineering Summer Meeting, Montreal, Canada.

[7] Gaster, M., 1969, "Vortex shedding from slender cones at low Reynolds numbers," Journal of Fluid Mechanics **38**, pp. 565-576.

[8] Ayoub, A., and Karamcheti, K., 1982, "An experiment on the flow past a finite circular cylinder at high subcritical and supercritical Reynolds numbers," Journal of Fluid Mechanics **118**, pp. 1-26.

[9] Williamson, C.H.K., 1992, "The natural and forced formation of spot-like 'vortex dislocations' in the transition of a wake," Journal of Fluid Mechanics **243**, pp. 393-441.

[10] Nakamura, H., Igarashi, T., 2008, "Omnidirectional reductions in drag and fluctuating forces for a circular cylinder by attaching rings," Journal of Wind Engineering and Industrial Aerodynamics **96**, pp. 887-899.

[11] Zdravkovich, M.M., Brand, V.P., Mathew, G., and Weston, A., 1998 "Flow past short circular cylinders with two free ends," Journal of Fluid Mechanics **203**, pp. 557-575.

[12] Inoue, O., and Sakuragi, A., 2008, "Vortex shedding from a circular cylinder of finite length at low Reynolds numbers," Physics of Fluids **20**, 033601.

[13] West, G.H., and Fox, T.A., 1990, "On the use of end plates with circular cylinders," Experiments in Fluids **9**, pp. 237-239.

[14] Lian, Q.X., and Su, T.C., "The Application of Hydrogen Bubble Method in the Investigation of Complex Flows," Atlas of Flow Visualization II, CRC, Boca Raton, FL.

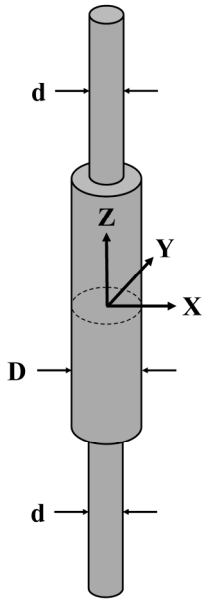

FIG 1. DIAGRAM OF THE DUAL STEP CYLINDER.

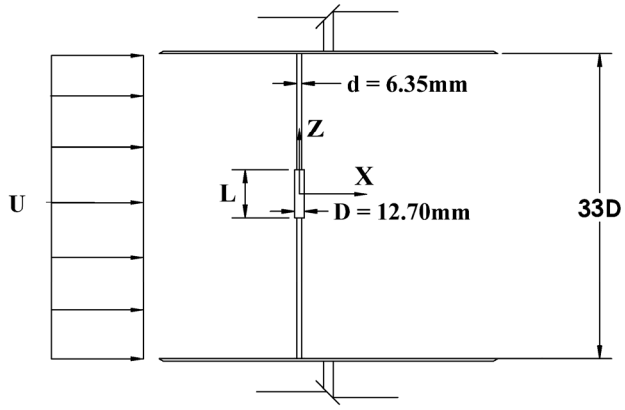

FIG 2. EXPERIMENTAL ARRANGEMENT.

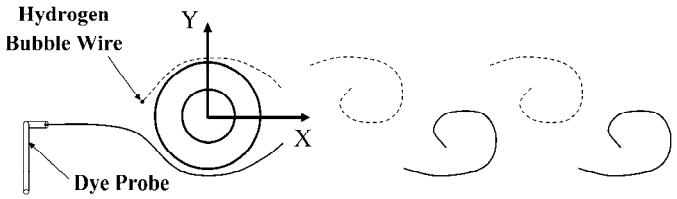

FIG 3. FLOW VISUALIZATION SETUP.

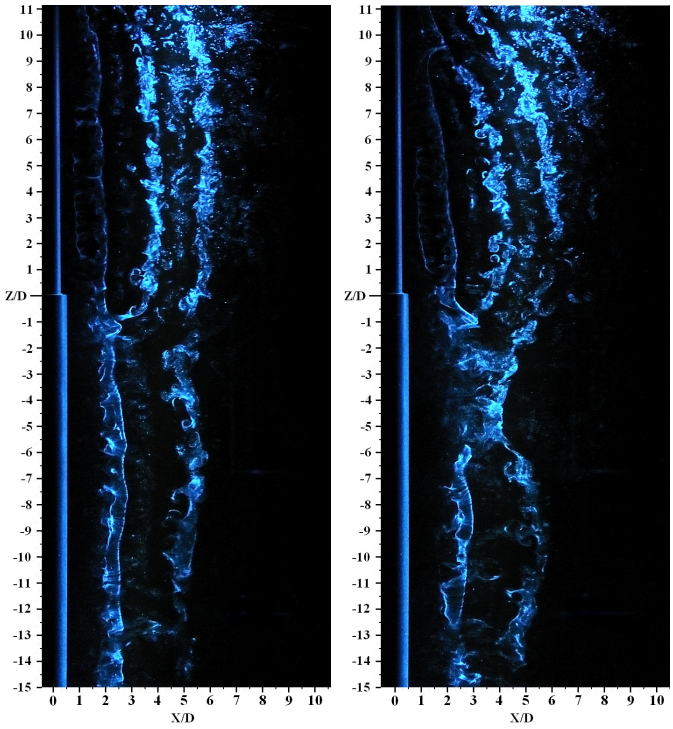

(a) Re_D = 1050, D/d = 2 (b) Re_D = 1050, D/d = 2

FIG 4. VORTEX SHEDDING IN THE WAKE OF A SINGLE STEP CYLINDER [6].

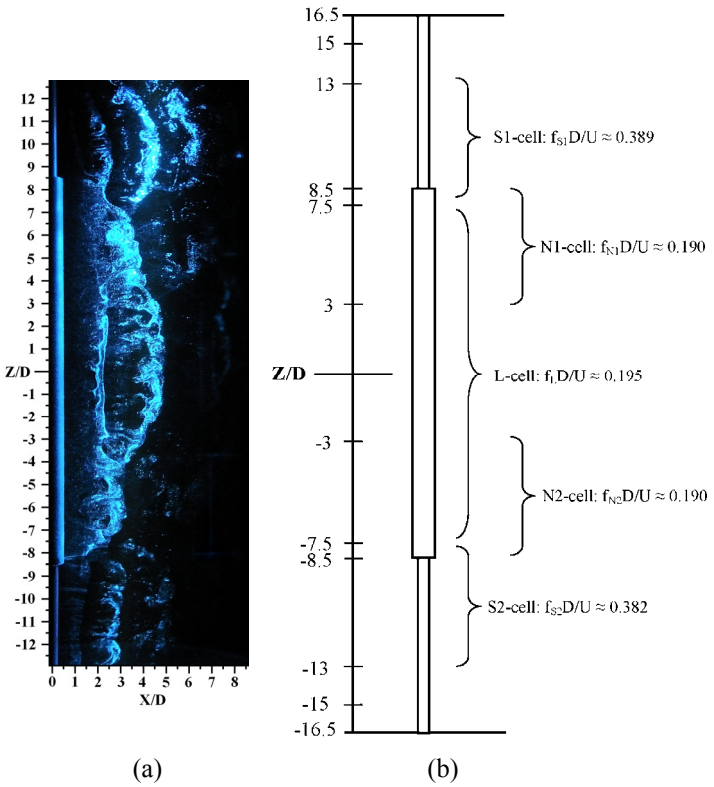

(a) (b)

FIG 5. VORTEX SHEDDING IN THE WAKE OF A DUAL STEP CYLINDER FOR L/D = 17.

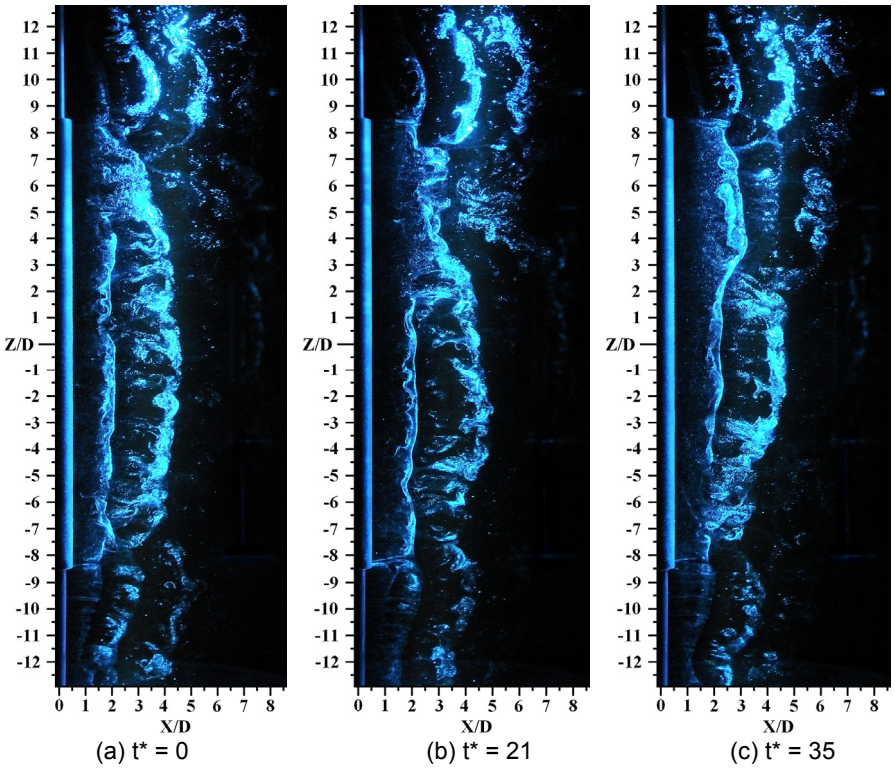

(a) t* = 0 (b) t* = 21 (c) t* = 35

FIG 6. N1-CELL DEVELOPMENT IN THE WAKE OF A DUAL STEP CYLINDER FOR L/D = 17.

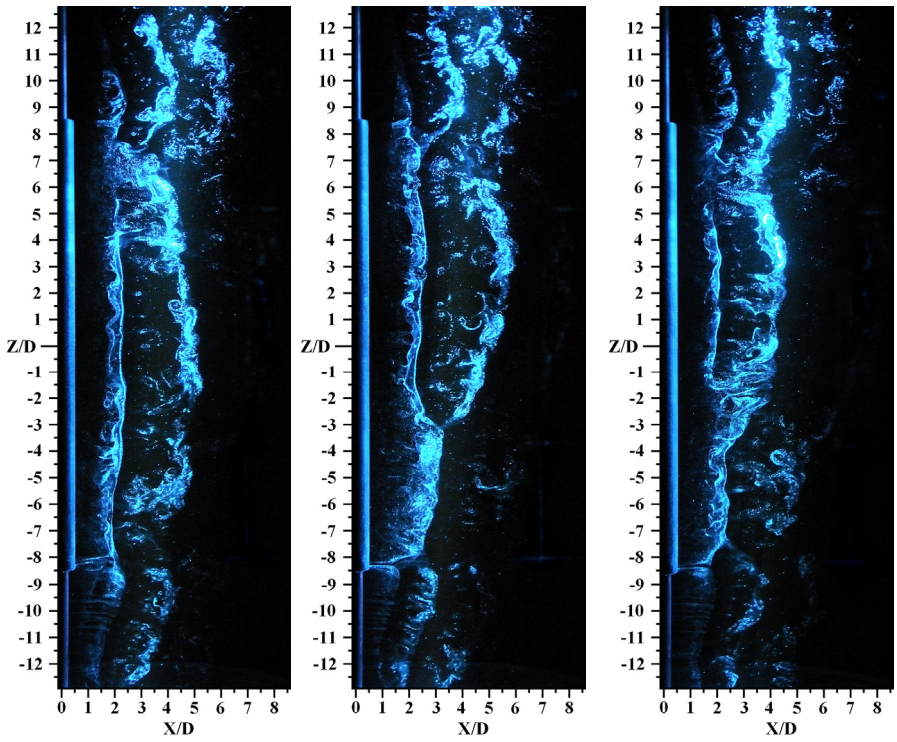

(a) t* = 0 (b) t* = 26.4 (c) t* = 37

FIG 7. N2-CELL DEVELOPMENT IN THE WAKE OF A DUAL STEP CYLINDER FOR L/D = 17.

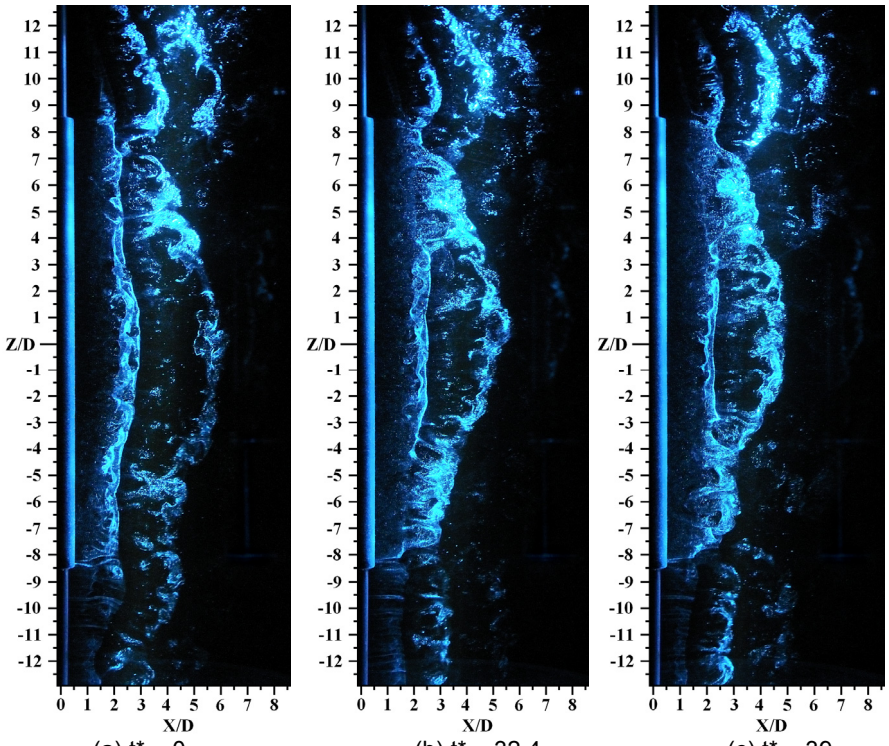

(a) t* = 0 (b) t* = 32.4 (c) t* = 39

FIG 8. N1 AND N2-CELL DEVELOPMENT IN THE WAKE OF A DUAL STEP CYLINDER FOR L/D = 17.

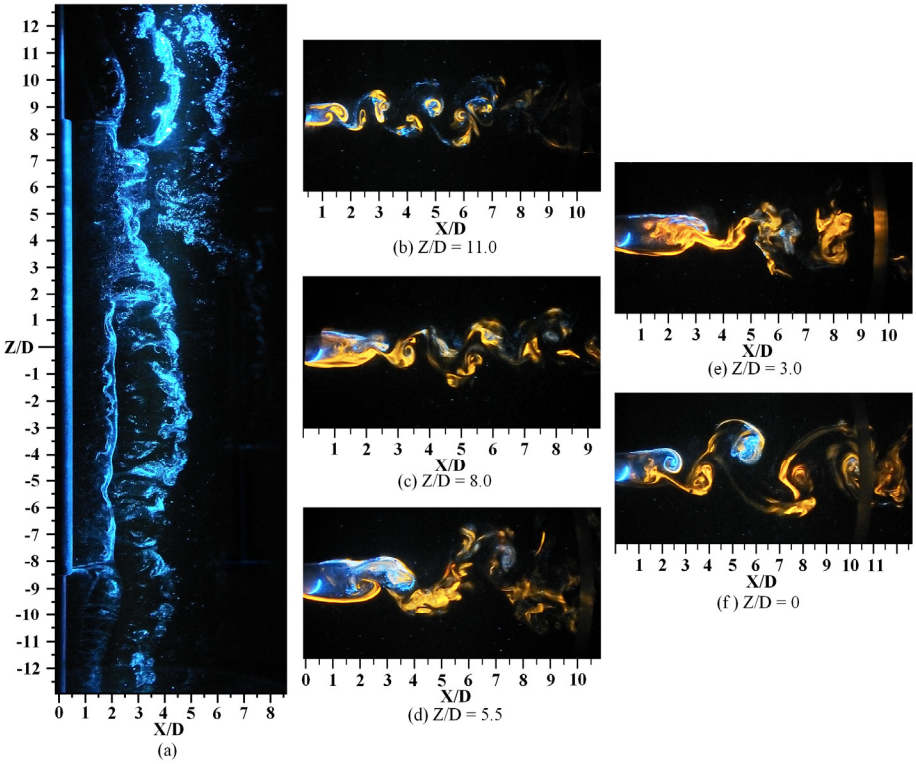

FIG 9. CHANGES IN THE VORTEX SHEDDING PATTERN ALONG THE SPAN OF A DUAL STEP CYLINDER FOR L/D = 17.

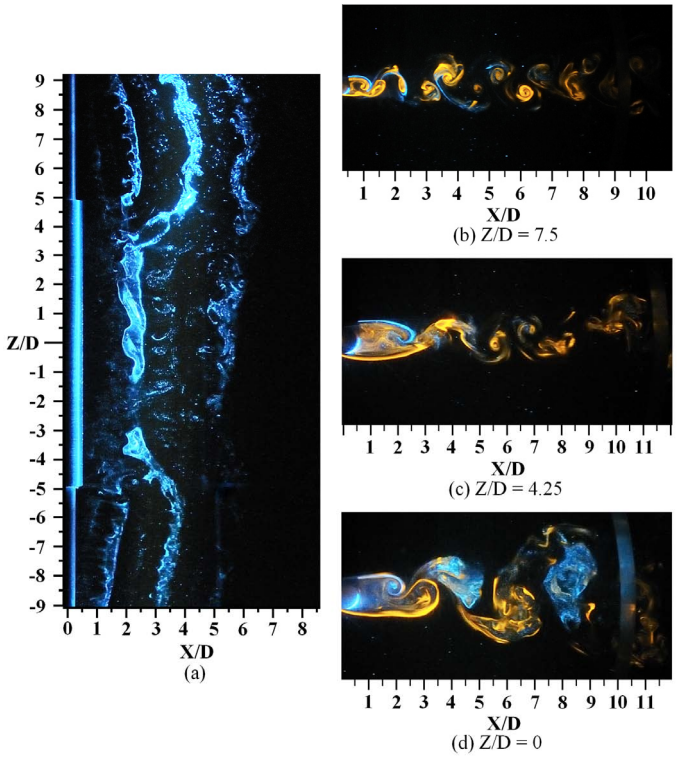

FIG 10. CHANGES IN THE VORTEX SHEDDING PATTERN ALONG THE SPAN OF A DUAL STEP CYLINDER FOR L/D = 10.

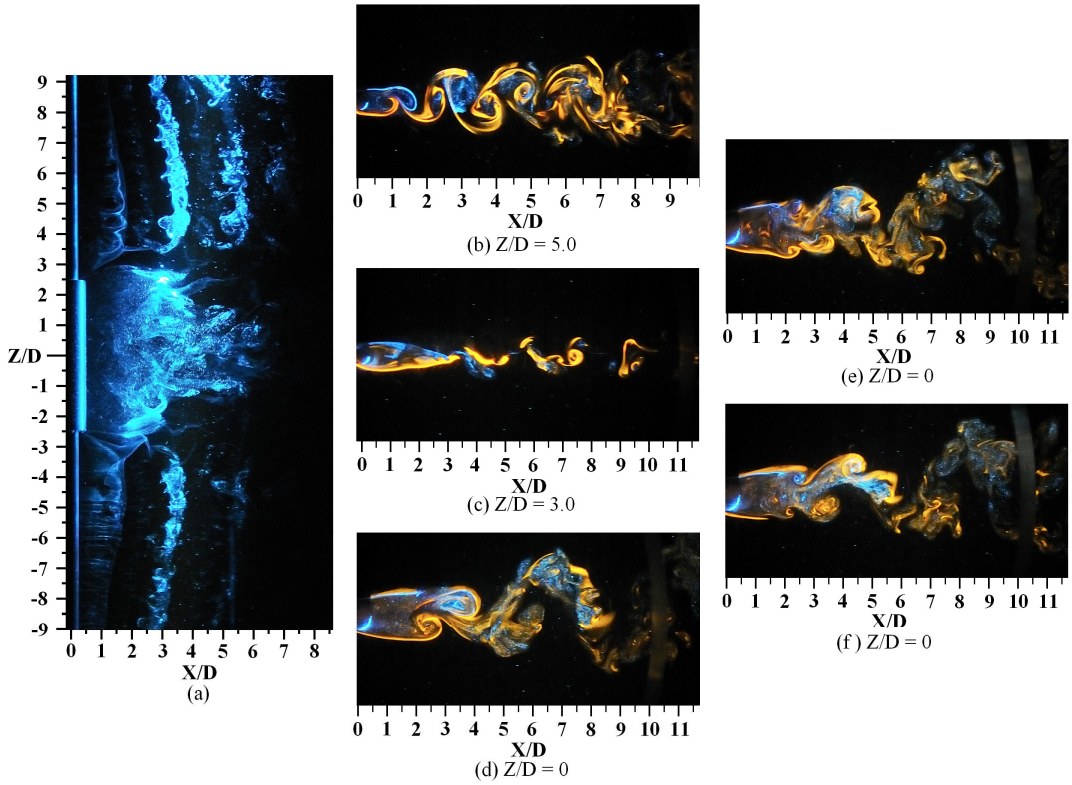

FIG 11. CHANGES IN THE VORTEX SHEDDING PATTERN ALONG THE SPAN OF A DUAL STEP CYLINDER FOR L/D = 5.

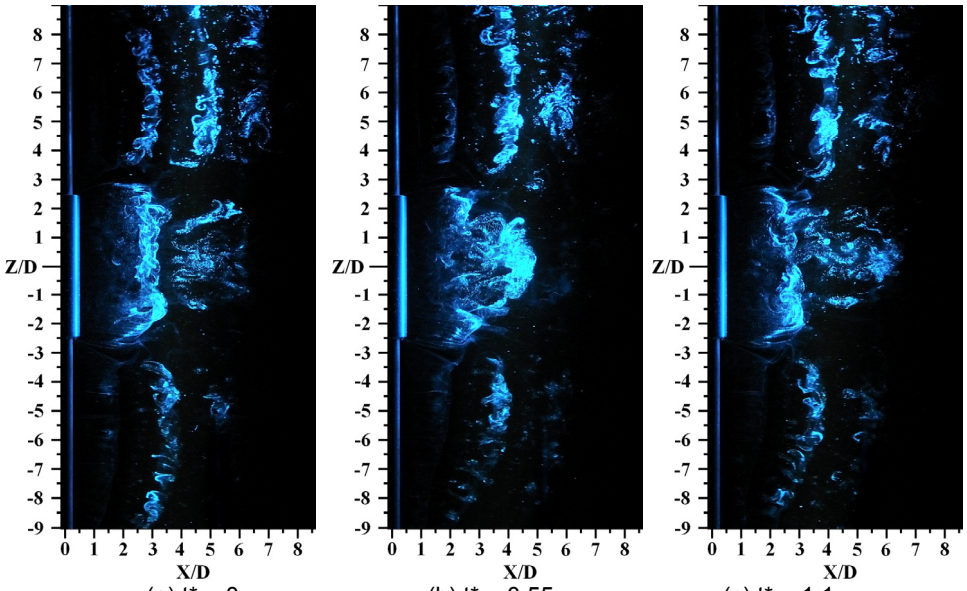

FIG 12. THREE-DIMENSIONAL SHEDDING IN THE WAKE OF A DUAL STEP CYLINDER FOR L/D = 5. IN CONTRAST TO OTHER FLOW IMAGES, POSITIONING THE LASER SHEET AT Y/D = 0.75 ALLOWS VISUALIZING VORTICES IN THE LARGE CYLINDER WAKE.

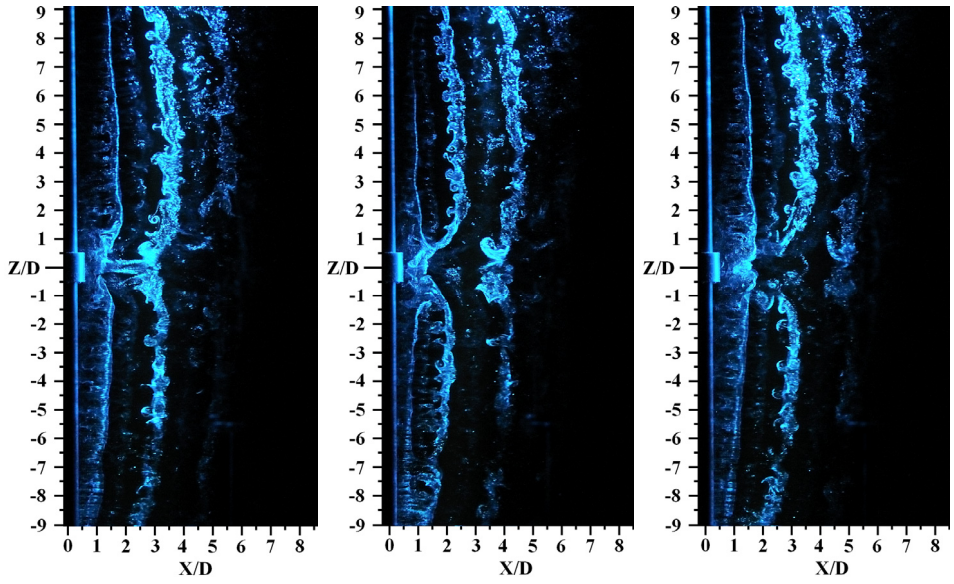

FIG 13. VORTEX SHEDDING IN THE WAKE OF A DUAL STEP CYLINDER FOR L/D = 1.

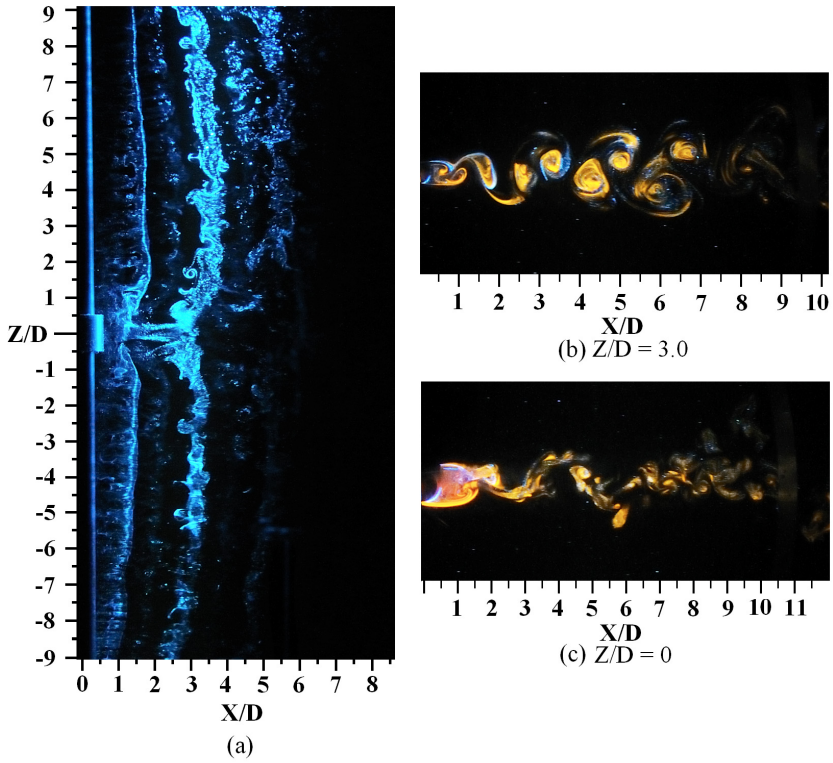

FIG 14. CHANGES IN THE VORTEX SHEDDING PATTERN ALONG THE SPAN OF A DUAL STEP CYLINDER FOR L/D = 1.